CONF-8905118--13

SAND--89-1764C

DE90 003484

2nd International Conference on
"Trends in Welding Research"
May 14-18, 1989, Gatlinburg,TN

HEAT TREATMENT OF PULSED Nd: YAG LASER WELDS IN A TI-14.8 WT.% AL-21.3 WT.%NB TITANIUM ALUMINIDE

W. A. Baeslack III
Department of Welding Engineering
The Ohio State University
Columbus, OH 43210

M. J. Cieslak and T. J. Headley
Sandia National Laboratories
Albuquerque, NM 87185

ABSTRACT

The influence of postweld heat treatment (PWHT) on the structure, mechanical properties and fracture characteristics of pulsed, Nd: YAG laser welds in a Ti-14.8 wt.% Al-21.3 wt.% Nb titanium aluminide has been investigated. Significant microstructure variations within the fusion zone (FZ) of all heat-treated welds were attributed primarily to the influence of local compositional fluctuations on decomposition of the metastable-β microstructure present in the as-welded FZ. An increase in PWHT temperature promoted a decrease in the maximum FZ hardness and an increase in the longitudinal-weld bend ductility. Correspondingly, the proportion of ductile tearing to cleavage fracture within the FZ increased with an increase in PWHT temperature.

TITANIUM ALUMINIDES REPRESENT a relatively new class of aerospace materials designed to provide superior elevated-temperature strength and creep properties and improved oxidation resistance versus conventional titanium alloys. Ti-13.5 wt.% Al-21.5 wt.% Nb (Ti-14 at.% Al-11 at.% Nb) is a first generation α_2 titanium aluminide which has experienced extensive metallurgical investigation in recent years [1]. Weldability studies performed on this alloy have shown that the weld structure and mechanical properties are extremely sensitive to weld cooling rate [2]. Cooling rates experienced during conventional arc welding, such as gas tungsten-arc welding and plasma-arc welding, were observed to promote the formation of fine, acicular α_2 microstructures which exhibited a high hardness (KHN 400-500) and low bend ductility (1-2%). The brittleness associated with these weld microstructures also led to cold cracking during weld cooling.

A recent investigation by the authors [3] demonstrated that pulsed Nd: YAG laser welding can generate relatively ductile (3-4% in bending), defect-free weldments in Ti-14.8 wt.% Al-21.3 wt.% Nb titanium aluminide sheet. The significant improvement in ductility over conventional arc weldments was attributed to the effect of high laser weld cooling rates in suppressing β decomposition to the brittle α_2 microstructures and instead promoting the formation of an ordered β superlattice.

Proposed applications for α_2 titanium aluminides in gas turbine-engine and airframe structural applications will require excursions to temperatures in the vicinity of 600 °C. Considering the metastable nature of the ordered β FZ microstructure, it is anticipated that such thermal excursions would promote β decomposition and thereby alter the mechanical properties of the weld zone. Indeed, the authors [4] have shown that heat treatment of the pulsed, Nd: YAG laser weld in Ti-14.8 wt.% Al-21.3 wt.% Nb sheet at a temperature of 565 °C/4 hours promoted β decomposition by the heterogeneous nucleation and growth of α_2 grains from β grain boundaries and decomposition of the intragranular regions to an extremely fine platelet α_2 structure. Predominance of the fine, platelet α_2 microstructure resulted in a high FZ hardness (KHN 450) and low bend ductility (about 1% in the as-welded condition). The fracture mode also changed from the nucleation and coalesence of equiaxed and elongated voids in the as-welded FZ to a distinctively cleavage mode of fracture following heat treatment.

Based on the aforementioned studies [3, 4], it is apparent that alternate post-weld heat treatments will be required to provide adequate laser weld ductilities in Ti-14.8 wt.% Al-21.3 wt.% Nb. Previous studies on conventional titanium alloy weldments have shown that an increase in PWHT temperature generally promotes microstructural coarsening with a corresponding improvement in weld ductility [5]. The purpose of the present investigation was to examine the influence of increased PWHT temperatures on the structure, mechanical properties and fracture characteristics of pulsed Nd: YAG laser weldments in a Ti-14.8 wt.% Al-21.3 wt.% Nb titanium aluminide.

EXPERIMENTAL PROCEDURE

Pulsed, Nd: YAG laser welds were produced in 75 mm x 10 mm coupons of 1.7 mm thick Ti-14.8 wt.% Al-21.3 wt.% Nb sheet. Compositional analysis of the α/β processed alloy indicated a trace of iron (0.065 wt.%) and low levels of oxygen and nitrogen (0.058 wt.% and 0.006 wt.%, respectively). Specific welding parameters utilized in this study were 20 Joules/pulse, 7.2 ms pulse duration, 10 pulses/s, 2.8 KW peak power, 4 mm/s travel rate (which provided an 80% weld overlap). Welding was performed with a 105 mm lens in a glove-box containing high purity argon to prevent atmospheric contamination.

Following laser welding, the coupons were vacuum heat treated (10^{-4} Pa) at 650, 750 and 850 °C for four hours and furnace cooled. The heat-treated coupons were subsequently sectioned, mounted in epoxy, polished down to 0.06 μm SiO_2 and etched with Kroll's reagent ($HF + HNO_3$) for characterization using differential interference contrast (DIC) light microscopy.

Analysis of weldment mechanical properties included the generation of Knoop microhardness traverses at two locations across the weld zone. Three-point progressive bend testing was also performed on longitudinal-weld oriented specimens with the top surface of the weld in tension. Fractographic examination of the weld zone was performed on an ETEC Autoscan scanning-electron microscope.

RESULTS & DISCUSSION

The light micrograph in Fig. 1a shows the uniform geometry of the laser weld FZ and the surrounding heat-affected zone (HAZ). Examination of the fusion boundary at increased magnification revealed the epitaxial growth of columnar β grains from the base metal substrate in toward the center of the FZ (Fig. 1b). Macrosegregation within the FZ was observed in the form of transverse solute banding. Primary solute bands originated from periodic changes in the solid-liquid interface velocity during pulsing of the laser heat source. Additional, secondary solute bands were attributed to minor fluctuations in the solid-liquid interface velocity during solidification of the individual melt zones. Although an extremely fine cellular-dendritic solidification substructure was observed within the columnar β grains, evidence of a transformed-β microstructure was not found. This analysis was consistent with the aforementioned TEM study [3] which showed the as-welded FZ to exhibit an ordered β microstructure with only occasional evidence of α_2 at β grain boundaries (Fig. 1c).

The light micrograph in Fig. 2a shows distinct structural variations within the FZ of the laser weld heat treated at 650 °C and their relation to the solute bands observed in Fig. 1. Examination of the FZ top (Fig. 2b) and bottom (Fig. 2c) at increased magnification revealed two principal microstructural features. Grain boundary allotriomorphs were observed to form a continuous network along prior-β grain boundaries. The growth of this "blocky-appearing" phase was appreciably more extensive in the bottom versus the top of the FZ. Intragranular regions not consumed by the grain boundary allotriomorphs exhibited an essentially featureless microstructure. It is of interest to note that the "U-shaped" intragranular region shown in Fig. 2c (arrow) which was not consumed by the grain boundary allotriomorphs appears to be associated with a primary solute band. Microstructural similarities between this FZ microstructure and that described for an identical laser weld heat-treated at 565 °C [4] suggest that the grain boundary phase was comprised of coarse α_2 grains and that the intragranular regions contained extremely fine α_2 platelets.

Microstructural differences within the laser weld FZ became increasingly apparent following heat treatment at 750 °C (Fig. 3). A dark-etching microstructure was predominant at the top of the FZ (Fig. 3b) and along solute bands in the center and bottom (Fig. 3c). Examination of this region at increased magnification suggested an extremely fine colony-type constituent comprised of α_2 and β phases. As shown in Fig. 3c, the location of a dark-etching, "U-shaped" band near the FZ bottom (arrow) paralleled the band of fine α_2 in the weld heat treated at 650 °C (indicated by arrow in Fig. 2c). A light-etching structure comprised of α_2 grains was present near the fusion boundaries and throughout the lower portion of the FZ.

The laser weld heat treated at 850 °C (Fig. 4a) exhibited a greater proportion of the dark-etching constituent. However, the macroscopic distributions of the dark and light-etching microstructures generally paralleled those of the welds heat treated at lower temperatures. Examination of the dark-etching constituent both at the top (Fig. 4b) and bottom (Fig. 4c) of the FZ revealed a coarser α_2 + β colony type structure and also the presence of fine, semi-continuous α_2 along prior-β grain boundaries.

Although limited in spatial resolution, light microscopy performed in the present study was useful in providing initial information regarding the influence of compositional variations in the laser weld FZ on the resulting transformed-β microstructure. Previous work has demonstrated that transverse solute banding can occur in titanium alloy weldments [6] and that it can markedly influence β decomposition [7]. In the present study, solute bands depleted in Al and enriched in Nb would be expected to promote transformation to the fine transformed structures (dark-etching) due to the increased β stability of these regions. The "U-shaped" solute bands indicated by arrows in the bottom of each FZ consistently exhibited such microstructures. Predominance of the fine α_2/β structure near the top of the FZ suggests that a depletion of the α_2-stabilizing element Al due to evaporation during laser welding may also influence the microstructure in this region. Indeed, electron microprobe analysis across the top surface of this laser weld has confirmed a depletion in Al content of 3 to 5 wt.% [8].

Microhardness traverses generated across the heat treated laser welds showed a negligible change in the base metal hardness versus the α/β processed sheet. However, PWHT did significantly increase the peak hardness within the weld FZ (Fig. 5). Consistent with the FZ microstructures described above, PWHT also promoted wide variations in hardness within the FZ. The highest FZ peak hardness of KHN 425 was located in the featureless intragranular regions of the laser weld heat treated at 650 °C. An appreciably lower hardness of KHN 260 was observed in the "blocky" α_2 microstructure predominant near the bottom of this FZ. PWHT at 750 °C reduced the maximum FZ hardness to KHN 355 in the fine colony α_2/β microstructure (dark-etching regions in light micrographs) present near the top of the FZ. A KHN of about 265 in the "blocky" α_2 structure was quite consistent with the similar microstructure observed in the weld heat treated at 650 °C. A coarsening of the colony α_2/β microstructure during PWHT at 850 °C resulted in a lower peak hardness of about KHN 325, while hardness in the "blocky" α_2 structure remained in the KHN 250-260 range. It is important to note that although peak hardness in the as-welded condition was found in the near-HAZ [1], peak hardnesses after PWHT were located exclusively within the FZ. Based on hardness traverses for all heat-treated weldments, it would be anticipated that tensile fracture across the weldments would occur exclusively in the unaffected base metal (i.e., 100% joint efficiency).

The results of the three-point bend tests on longitudinal-weld oriented specimens are shown in Fig. 6. Note that these data are for welds oriented parallel to the sheet rolling direction with the weld reinforcement

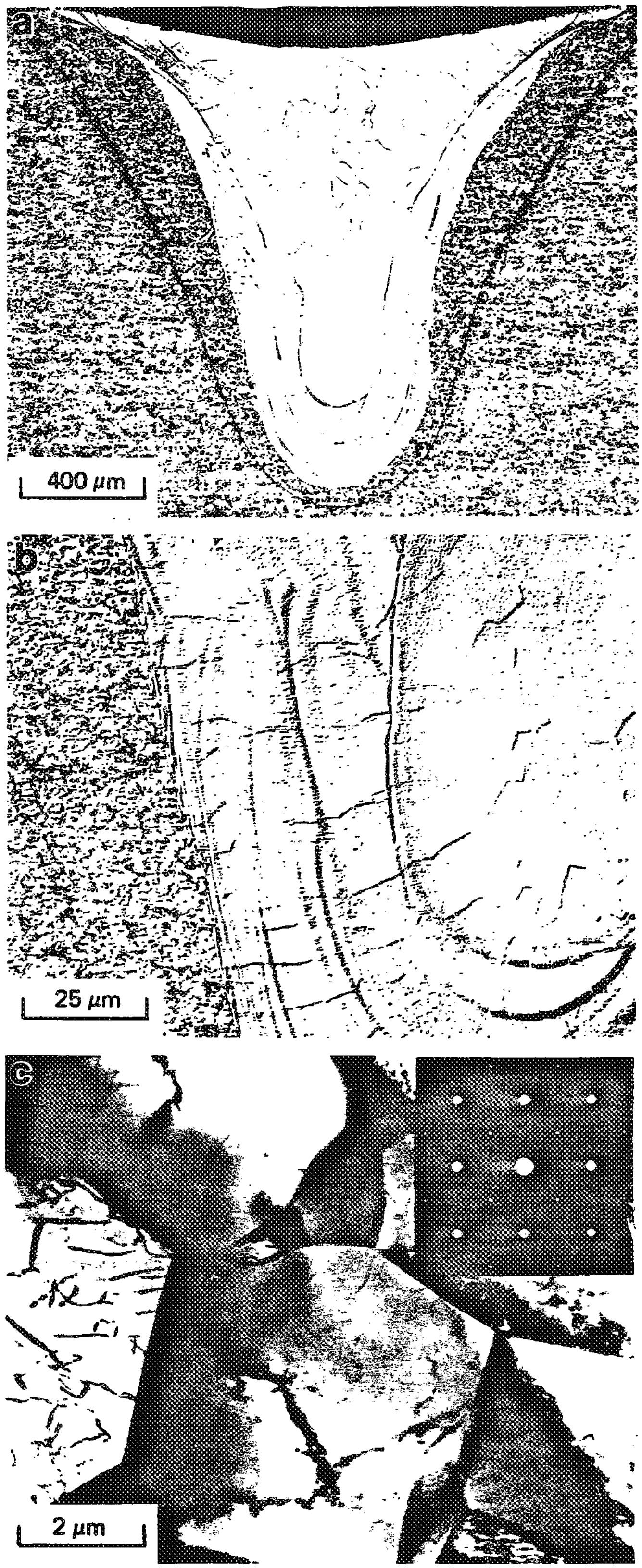

Fig. 1 - (a, b) Light micrographs (differential-interference contrast) and (c) TEM micrograph showing transverse sections of as-welded pulsed, Nd: YAG laser welds in Ti-14.8 wt.% Al-21.3 wt.% Nb sheet [1].

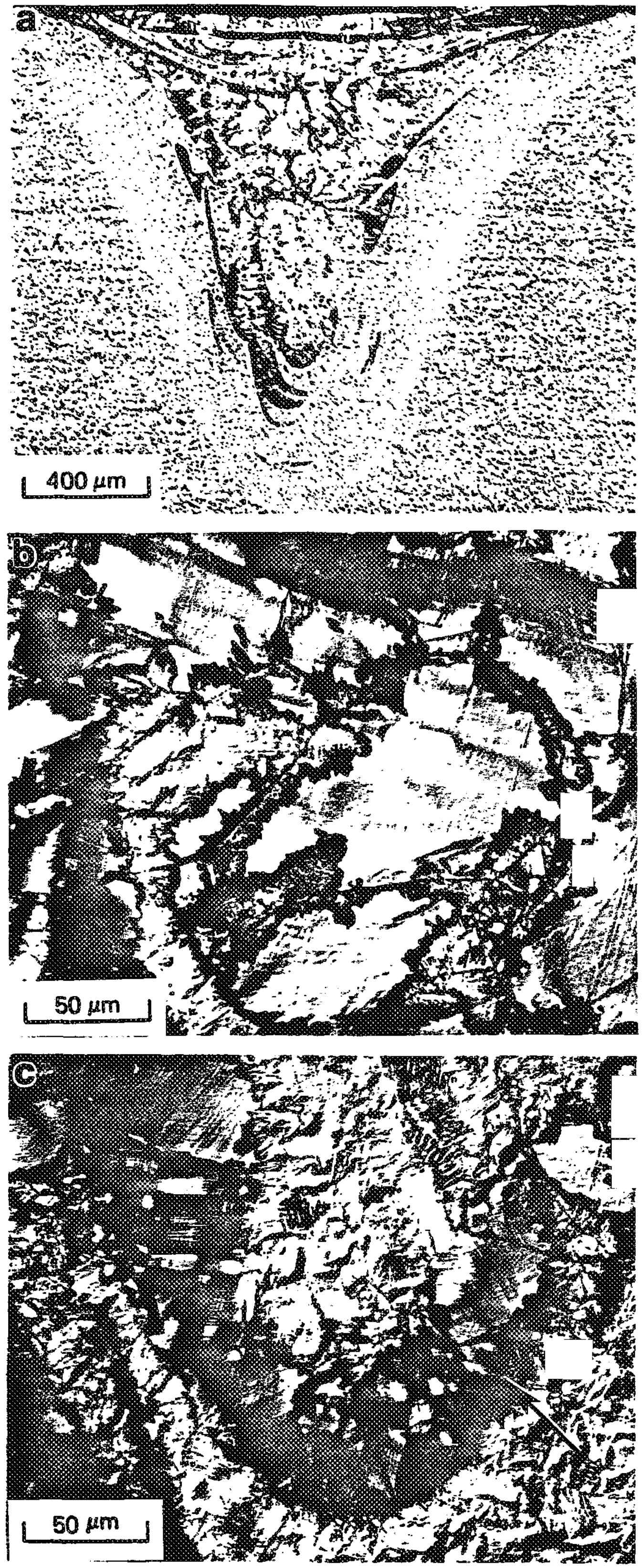

Fig. 2 - Light micrographs (differential-interference contrast) showing transverse sections of pulsed, Nd:YAG laser welds in Ti-14.8 wt.% Al-21.3 wt.% Nb sheet PWHT at 650 °C/4 hr FC.

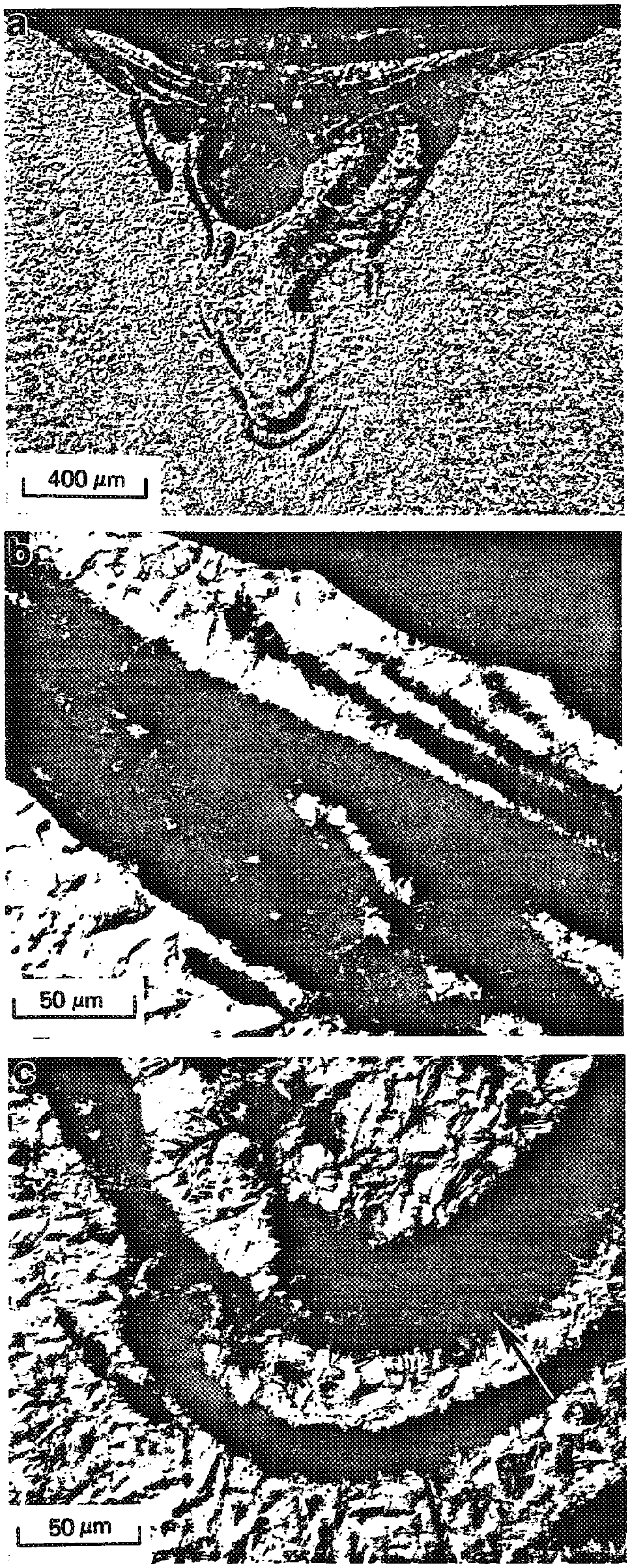

Fig. 3 - Light micrographs (differential-interference contrast) showing transverse sections of pulsed, Nd:YAG laser welds in Ti-14.8 wt.% Al-21.3 wt.% Nb sheet PWHT at 750 °C/4 hr FC.

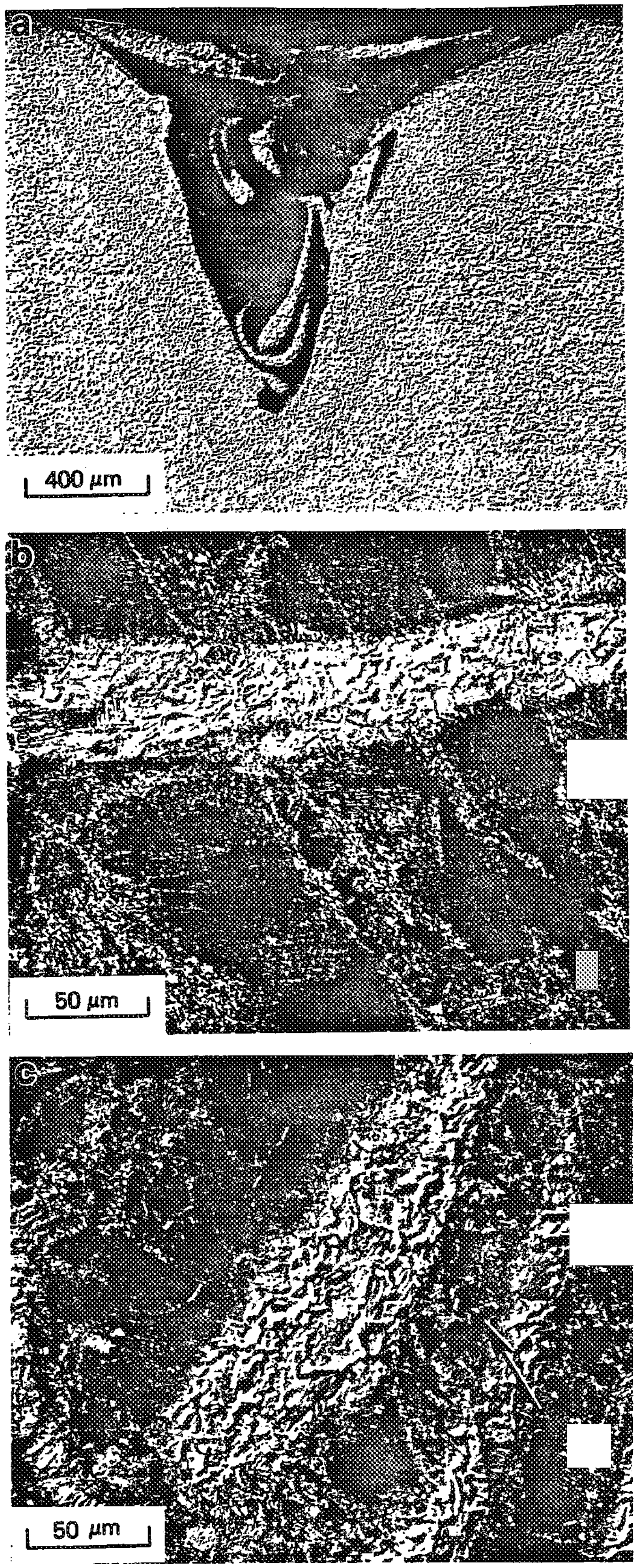

Fig. 4 - Light micrographs (differential-interference contrast) showing transverse sections of pulsed, Nd:YAG laser welds in Ti-14.8 wt.% Al-21.3 wt.% Nb sheet PWHT at 850 °C/4 hr FC.

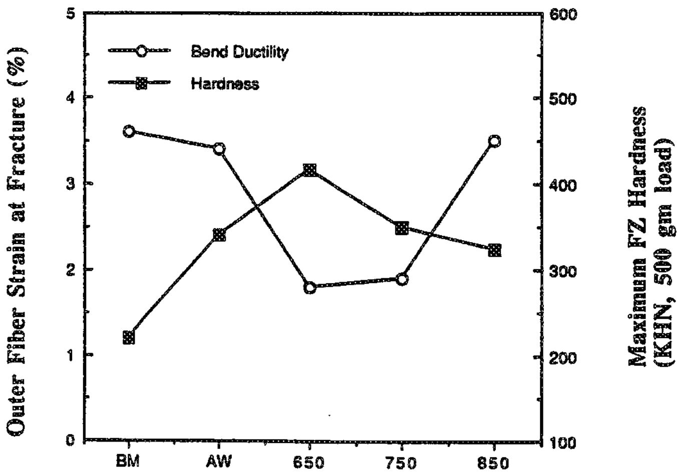

Fig. 5 - Plot of maximum FZ hardness and three- point bend ductility (elastic + plastic deformation) for Ti-14.8 wt.% Al-21.3 wt.% Nb base metal and longitudinal-weld oriented specimens in the as-welded and PWHT conditions.

removed by surface grinding. As indicated, PWHT at 650 °C and 750 °C promoted a reduction in bend ductility to about 2% (elastic + plastic strain) versus the as-welded condition. Utilization of the 850 °C PWHT temperature, however, restored bend ductility to near base metal levels.

Fracture in the weld FZ occurred predominantly transgranularly in both the as-welded and PWHT conditions (Fig. 6). Fracture of the as-welded FZ occurred by the nucleation and coalesence of both equiaxed and elongated voids. Near the top of the FZ (Fig. 6a), the surface appeared more faceted with occasional evidence of intergranular fracture. The observation of these surfaces at increased magnification revealed dimples of varying size and shape thus indicating microscopically ductile fracture. The center and bottom regions of the as-welded FZ exhibited both equiaxed dimples and elongated flutes (Fig. 6b). Despite the presence of a continuous α_2 network at the prior-β grain boundaries, fracture of the weldment heat treated at 650 °C occurred transgranularly by a cleavage fracture mode. Larger facets near the top of the FZ (Fig. 6c) versus the bottom (Fig. 6d) may be related to differences in the size and morphology of underlying prior-β grains. Increased evidence of ductile tearing was visible at the bottom portions of the FZ which exhibited primarily the "blocky" α_2 microstructure (Fig. 6d). Since ductile tearing in α_2 titanium aluminides is generally associated with the presence of the β phase, this observation suggests that β phase may be present at α_2 grain boundaries. Indeed, the retention of the β phase would be expected if allotriomorph growth occurred by a diffusional process. Fracture of the weld heat treated at 750 °C appeared quite similar to that heat treated at 650 °C (Figs. 6e and 6f). Heat treatment at 850 °C, however, promoted fracture with smaller facet sizes and an increased proportion of ductile tearing in both the top and bottom regions of the weld FZ (Figs. 6g and 6h).

SUMMARY

Results of this investigation showed that the ductility of pulsed, Nd: YAG welds in a Ti-14.8 wt.% Al-21.3 wt.% Nb titanium aluminide increase with increasing PWHT temperature, with a bend ductility following PWHT at 850 °C being nearly equivalent to that of the α/β processed base material. Significant variations in microstructure and hardness within the heat-treated fusion zones were attributed to compositional fluctuations associated with pulsed laser welding.

REFERENCES

1) Rhodes, C. G., Hamilton, C. H., and Paton, N. E., AFML-TR-78-130, (1978).
2) Mascorella, T., and Baeslack, W. A. III., "Weldability of a Ti-14 wt.% Al-21 wt.% Nb Titanium Aluminide," to be published in the Welding Journal Research Supplement.
3) Baeslack, W. A. III., Cieslak, M. J., and Headley, T. J., Scripta Metallurgica, 22, 1155-1160 (1988).
4) Baeslack, W. A. III., and Cieslak, M. J., "Effect of Heat Treatment on the Structure, Properties and Fracture of Pulsed Nd: YAG Laser Welded Ti-14.8 wt.% Al-21.3 wt.% Nb," to be published in Scripta Metallurgica.
5) Baeslack, W. A. III., Becker, D. W., and Froes, F. H., J. Metals, 36, 46-58 (1984).
6) D'Annessa, A. T., Welding J. 45, 569s-576s, (1966).
7) Baeslack, W. A. III., J. Matls. Sci. Letters, 1, 229-231, (1982).
8) Cieslak, M. J., Unpublished Research, Sandia National Laboratories, Albuquerque, NM, (1988).

ACKNOWLEDGEMENTS

The authors wish to thank GE Aircraft, Cincinnati, OH for providing the titanium-aluminide sheet. Appreciation is also expressed to Mr. Thomas Lienert of Sandia National Laboratories, Mr. Mark Dodd of the Metcut Materials Group at the Wright Research and Development Center, WPAFB, OH and Mr. Anthony Cox of The Ohio State University for their valuable technical assistance. Work performed at Sandia National Laboratories was supported by the Department of Energy under contract # DE-AC04-76DP00789.

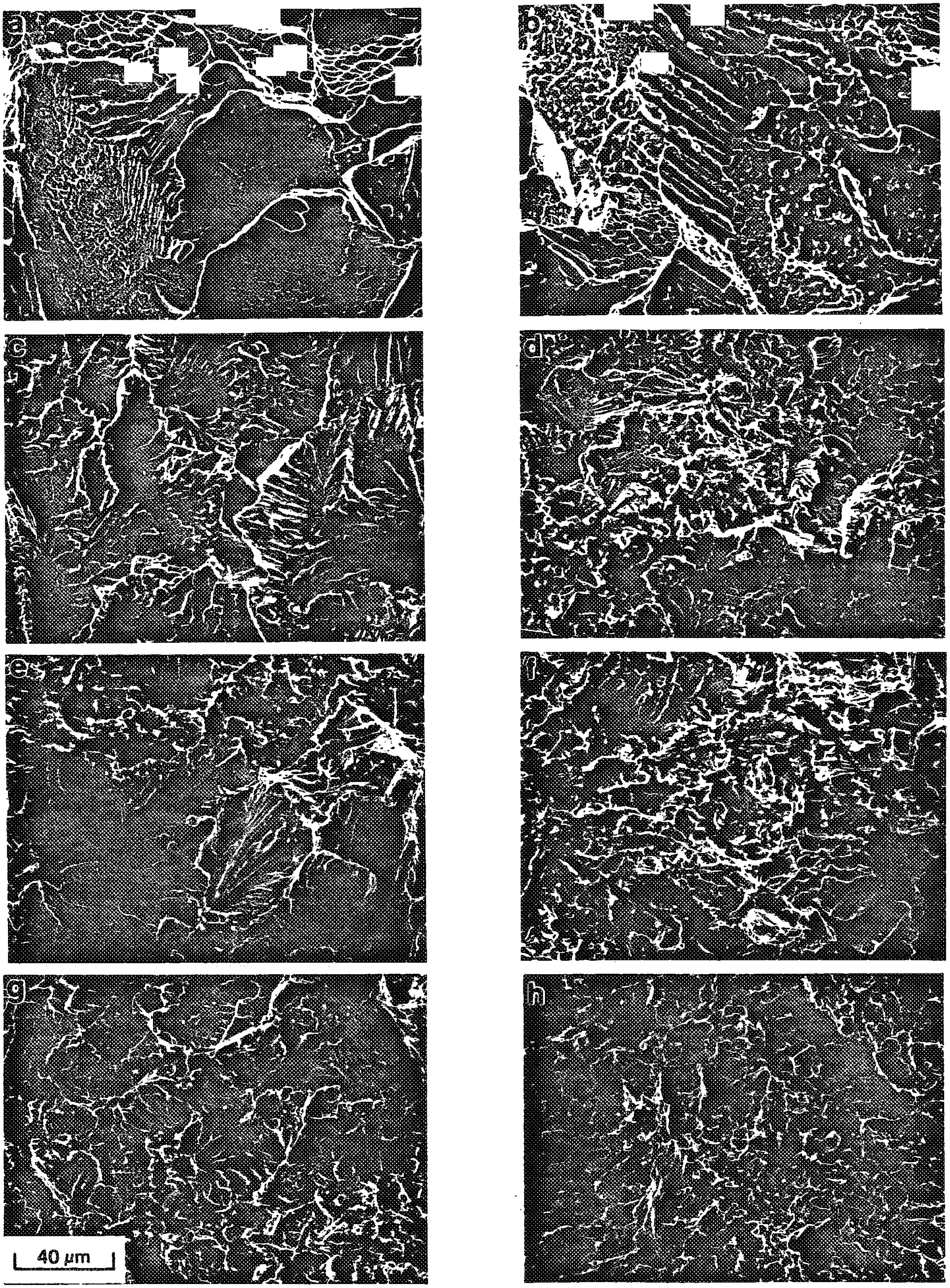

Fig. 6 - SEM fractographs of longitudinal-weld oriented bend specimens in pulsed, Nd: YAG laser welds in Ti-14.8 wt.% Al-21.3 wt.% Nb sheet : (a, b) as welded; (c, d) PWHT at 650 °C/4 hr FC; (e, f) PWHT at 750 °C/4 hr FC; (g, h) PWHT at 850 °C/4 hr FC. Fracture surfaces shown in left-hand column are located at top of weld fusion zone, fractographs in right-hand column are located at bottom of fusion zone.